

LIMIT STRESS SPLINE MODELS FOR GRP COMPOSITES

ENGR. DR. CHUKWUTOO C. IHUEZE (B.ENG., M.ENG., Ph.D)

*Department of Mechanical Engineering, Anambra State
University of Science and Technology, Uli*

ABSTRACT

This paper focuses on the use of Spline functions in modelling the critical stress - strain responses of polyester matrix GRP Composites. Spline functions were established on the assumption of three intervals and fitting of quadratic and cubic splines to critical stress-strain responses data. Quadratic and Cubic spline models for three intervals of data points $0.024 \leq x \leq 0.036$, $0.036 \leq x \leq 0.061$ and $0.061 \leq x \leq 0.12$ were established. The optimization of quadratic and cubic models by gradient search optimization gave the critical strain as 0.024, which resulted to strength of approximately 26 MPa. Strain hardening was observed to occur within a strain range of 0.03 to 0.12 leading to strength of about 62 MPa predicted by Cubic spline. Splines were found to accurately predict the functional values at subinterval, $0.024 \leq x \leq 0.036$ of data points. Spline model is therefore recommended as it evaluates the function at subintervals, eliminating the error associated with wide range interpolation.

Keywords: *Spline Models; Limit stress; Natural splines; Composite Matrix; GRP.*

1. INTRODUCTION

The strength of any material used in any design is very important in order to evaluate the performance index of a particular project. Plastics are polymers that are viscoelastic in nature, show time dependence response to applied stress (Creep), [1]. GRP mechanical properties are therefore affected by creep parameters. Budiansky and Fleck [2], Chung and Weitsmann [3] and Hsu et al [4] all working on compressive failure of GRP composites reported the compressive kinking failure of GRP composites, which usually occurs within the materials elastic limit. Ihueze [5] reported the buckling response of GRP composites due to random material properties of GRP composites resulting from geometric inhomogeneity. This resulted to the nonlinear models of the study. Above all plastics have high strength to weight ratio when compared to the conventional metal material, Wood [6] and Foye [7]. This is why

plastics or plastic composites are used in lightweight structures as found in aircraft, aeroplane, modern automobiles, boats, ships, etc. Classical reports on the strength of plastic composites show that buckling is a limiting factor in the selection of plastics as a design material, Eneteanya and Ihueze [8], reported that the compressive strength of plastic composite could be

lower than 50% of its tensile strength. This article focuses on the development of line models that predict the limiting stresses of the commonly used polyester matrix GRP composites made by hand lay-up.

2 THEORETICAL ANALYSIS (REVIEW)

2.1 Existing Model on Aligned Polymer Composite Strength. Compressive failure of GRP composites manifests as kinking failure. Kink bands are formed which are bounded by fiber breaks resulting from deformations

immediately following the attainment of the largest compressive load. This can limit the compressive strength of a composite material to a very low fraction of its tensile strength; a review of the studies on compressive kinking failures in aligned GRP mechanical composites is presented below.

a). Rosen's Overestimation Of Compression Strength.

The critical kinking strength S_c is given as

$$S_c = G \tag{1}$$

G = Shear modulus in the longitudinal direction

Rosen's equation has been shown by recent investigations to overestimate the actual

polymer matrix compression strength S_c by a factor of about four. Argon [9] combined the nonlinear plastic behavior (viscoelastic) of the composite material with the effects of fiber misalignment in his approximate equation for the kinking strength S_c as

$$S_c = S_{sy} / \phi \tag{2}$$

S_{sy} = Shear yield strength

f = The initial maximum misalignment of the fibres, in radian

Equation (2) Suggests that the yield strengths in shear, S , in combination S_{sy} in combination with initial fiber misalignments f are the most critical parameters affecting the compressive kinking strength of aligned FRP composites.

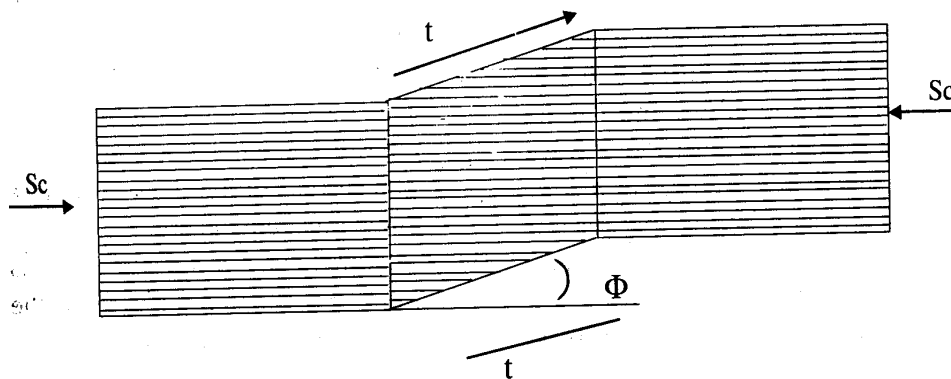


Fig. 1: Kink-Band.

(b) Ihueze [5] Regression Model

Ihueze [5] established a regression model to predict the critical stress-strain response polyester matrix GRP as

$$y_{cr} = 61.14 - 1873.59x + 16184.45x^2 \tag{3}$$

Where x_{cr} = critical strain, y_{cr} = critical stress
 This model is a second order polynomial model that fits the whole range of data. There may be danger of over approximation of function as seen in fig. 2. Spline model that fits a lower order polynomial to subset of data points is expected to improve the predictions.

2.2 Polynomial Interpolation

Polynomial regression is used to fit data

points of experimental results. The general interpolating polynomial is expressed as:

$$p_n(x) = a_0 + a_1x_i + a_2x_i^2 + a_3x_i^3 + \dots + a_nx_i^n \tag{4}$$

Where

$a_0 - a_n$ = polynomial coefficients or constants

X_i = independent variables.

n = polynomial order.

$P_n(x)$ = dependent variable(parameter)

Interpolation with higher order polynomial is supposed to improve the accuracy of results but this is not always true. The accuracy of higher order polynomial fit may be low because of numerical errors associated with

many computations associated and overshoot of polynomials around data points. Meandering of polynomials around data is a characteristic of higher order polynomial fit. Numerical instability is therefore associated with higher order polynomial fit.

Kreys Zig [10] reported the work of Schoenberg who presented the idea of fitting lower order polynomials (splines) to subintervals of data point. The idea of spline is that instead of fitting a higher order polynomial to data points, fitting is done at subintervals. The lower order polynomials for the subintervals are called splines or spline functions. There are linear, quadratic and cubic splines. Cubic spline is classically recommended. The cubic polynomial to fit the subinterval of data points is expressed by Canale and Chapra [11] as

$$f_i(X) = a_i X^3 + b_i X^2 + c_i X + d_i \quad (5)$$

Where $f_i((x) =$ parameter.

2.2.1 Derivation of Cubic Spline Equation.

The basic assumptions to be used are:

1. The value of the functions must be equal at the interior knots (nodes).
2. The first and last functions must pass through the end nodes.
3. The first derivations of the functions at the interior knots (nodes) must be equal.
4. The second derivations at the interior knots must be equal.
5. The second derivatives at the end knots must equal zero.

We therefore have five spline conditions to exploit. Fig. 2 is now used with the above five conditions as:

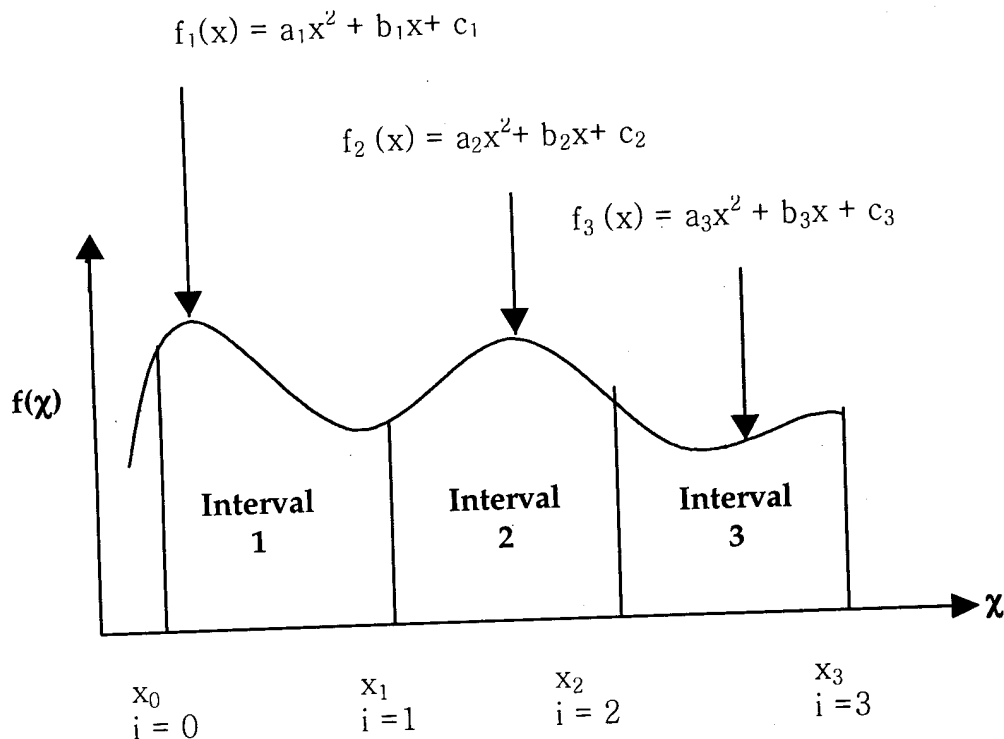


Fig. 2. Notation for the derivation of cubic spline (notice that there are n intervals and n+1 data points).

Employing the five conditions above we have the following equations:

Using the first condition, fig.2 and interior knots:

$$a_1 X_1^3 + b_1 X_1^2 + c_1 X_1 + d_1 = f(X_1) \quad (6)$$

$$a_2 X_1^3 + b_2 X_1^2 + c_2 X_1 + d_2 = f(X_1) \quad (7)$$

$$a_2 X_2^3 + b_2 X_2^2 + c_2 X_2 + d_2 = f(X_2) \quad (8)$$

$$a_3 X_2^3 + b_3 X_2^2 + c_3 X_2 + d_3 = f(X_2) \quad (9)$$

Using the second condition, fig.2 and end

knots:

$$a_1X_0^3 + b_1X_0^2 + c_1X_0 + d_1 = f(X_0) \quad (10)$$

$$a_3X_3^3 + b_3X_3^2 + c_3X_3 + d_3 = f(X_3) \quad (11)$$

Using the third condition, fig.2 and interior knots:

$$3a_1X_1^2 + 2b_1X_1 + c_1 - 3a_2X_1^2 - 2b_2X_1 - c_2 = 0 \quad (12)$$

$$3a_2X_2^2 + 2b_2X_2 + c_2 - 3a_3X_2^2 - 2b_3X_2 - c_3 = 0 \quad (13)$$

Using the fourth condition, fig.2 and interior knots:

$$6a_1X_1 + 2b_1 - 6a_2X_1 - 2b_2 = 0 \quad (14)$$

$$6a_2X_2 + 2b_2 - 6a_3X_2 - 2b_3 = 0 \quad (15)$$

Using the fifth condition, fig.2 and interior knots:

$$6a_1X_0 + 2b_1 = 0 \quad (16)$$

$$6a_3X_3 + 2b_3 = 0 \quad (17)$$

The associated polynomial constants to be estimated are the a's, b's, c's and d's which are twelve in number which require twelve equations that are satisfied by Eq. (6) - (17).

By putting Eq. (6) - (17) in matrix form,

$$\begin{pmatrix} x_1^3 & x_1^2 & x_1 & 1 & 0 & 0 & 0 & 0 & 0 & 0 & 0 & 0 \\ 0 & 0 & 0 & 0 & x_1^3 & x_1^2 & x_1 & 1 & 0 & 0 & 0 & 0 \\ 0 & 0 & 0 & 0 & x_2^3 & -x_2^2 & x_2 & 1 & 0 & 0 & 0 & 0 \\ 0 & 0 & 0 & 0 & 0 & 0 & 0 & 0 & x_2^3 & x_2^2 & x_2 & 1 \\ x_0^3 & x_0^2 & x_0 & 1 & 0 & 0 & 0 & 0 & 0 & 0 & 0 & 0 \\ 0 & 0 & 0 & 0 & 0 & 0 & 0 & 0 & x_3^3 & x_3^2 & x_3 & 1 \\ 3x_1^2 & 2x_1 & 1 & -3x_1^2 & -2x_1 & -1 & 0 & 0 & 0 & 0 & 0 & 0 \\ 0 & 0 & 0 & 0 & 3x_2^2 & 2x_2 & 1 & -3x_2^2 & -2x_2 & -1 & 0 & 0 \\ 6x_1 & 2 & 0 & 0 & -6x_1 & -2 & 0 & 0 & 0 & 0 & 0 & 0 \\ 0 & 0 & 0 & 0 & 6x_2 & 2 & 0 & 0 & -6x_2 & -2 & 0 & 0 \\ 6x_0 & 2 & 0 & 0 & 0 & 0 & 0 & 0 & 0 & 0 & 0 & 0 \\ 0 & 0 & 0 & 0 & 0 & 0 & 0 & 0 & 6x_3 & 2 & 0 & 0 \end{pmatrix} \begin{pmatrix} a \\ b_1 \\ c_1 \\ d_1 \\ a_2 \\ b_2 \\ c_2 \\ d_2 \\ a_3 \\ b_3 \\ c_3 \\ d_3 \end{pmatrix} = \begin{pmatrix} f(x_1) \\ f(x_1) \\ f(x_2) \\ f(x_2) \\ f(x_0) \\ f(x_3) \\ 0 \\ 0 \\ 0 \\ 0 \\ 0 \\ 0 \end{pmatrix}$$

Before the above system is solved, it is important to rearrange the equations to avoid zero elements in the leading diagonal of the matrix. This guarantees the success of division with zero when applying Gauss-Jordan elimination method with pivoting.

2.2.2 Derivation of Quadratic Spline

The objective of quadratic spline is to fit second order polynomials to data points within intervals as specified in Fig. 3. The quadratic interpolation polynomial can be expressed as:

$$f_i(X) = a_iX^2 + b_iX + c_i \quad (18)$$

From fig.3, values at the knots within the interval $X_0 \leq x \leq X_1$ with subintervals: $X_0 \leq x \leq X_1$, $X_1 \leq x \leq X_2$, $X_2 \leq x \leq X_3$. Eq (18) gives three unknowns for each interval and therefore nine unknowns for the three intervals. Therefore for quadratic spline constants, 3n equations for the 3n unknowns are required, where n stands for number of intervals. The conditions that lead to nine equations are:

1. The value of the functions must be equal at the interior knots (nodes).

2. The first and last functions must pass through the end nodes.
3. The first derivatives of the functions at the interior knots (nodes) must be equal.
4. The second derivative of the function at the first point is zero because of natural spline conditions that suggests that the spline is linear at the first and endpoints.

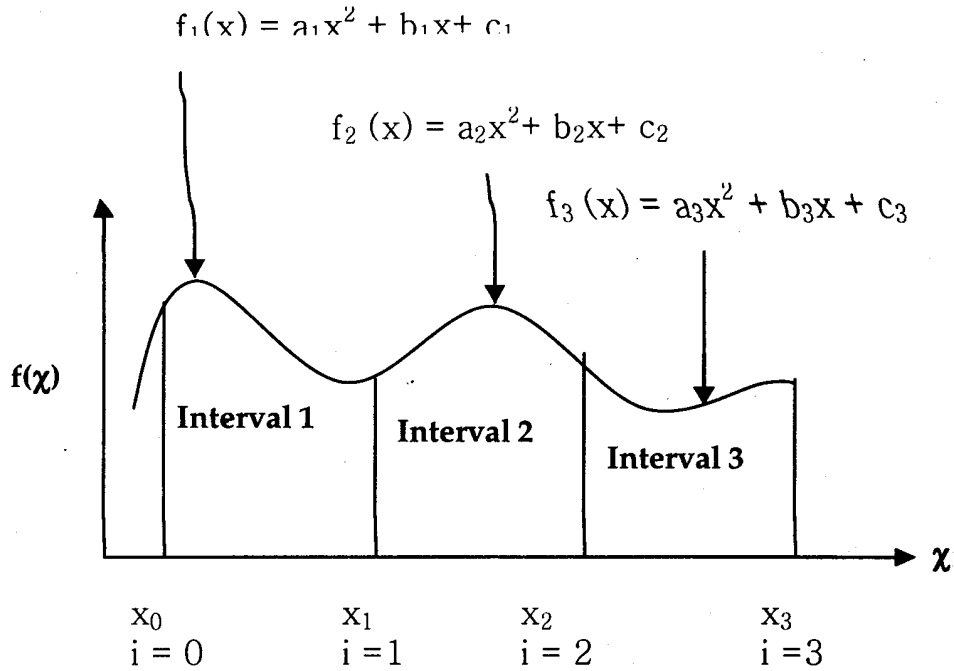


Fig. 3: Notations for quadratic spline using three intervals.

Now employing the four conditions above, the following system of equations results.

Using the first condition: -

$$a_1 X_1^2 + b_1 X_1 + c_1 = f(X_1) \quad (19)$$

$$a_2 X_1^2 + b_2 X_1 + c_2 = f(X_2) \quad (20)$$

$$a_2 X_2^2 + b_2 X_2 + c_2 = f(X_2) \quad (21)$$

$$a_3 X_2^2 + b_3 X_2 + c_3 = f(X_2) \quad (22)$$

Using the second condition: -

$$a_1 X_0^2 + b_1 X_0 + c_1 = f(X_0) \quad (23)$$

$$a_3 X_3^2 + b_3 X_3 + c_3 = f(X_3) \quad (24)$$

Using the third condition: -

$$2a_1 X_1 + b_1 = 2a_2 X_1 + b_2 \quad (25)$$

$$2a_2 X_2 + b_2 = 2a_3 X_2 + b_3 \quad (26)$$

Using the fourth condition:

$$2a_1 = 0, a_1 = 0 \quad (27)$$

Putting the value $a_1 = 0$ in the above equations,

$$b_1 X_1 + c_1 = f(X_1) \quad (28)$$

$$a_2 X_1^2 + b_2 X_1 + c_2 = f(X_1) \quad (29)$$

$$a_2 X_2^2 + b_2 X_2 + c_2 = f(X_2) \quad (30)$$

$$a_3 X_2^2 + b_3 X_2 + c_3 = f(X_2) \quad (31)$$

$$b_1 X_0 + c_1 = f(X_0) \quad (32)$$

$$a_3 X_3^2 + b_3 X_3 + c_3 = f(X_3) \quad (33)$$

$$b_1 - 2a_2 X_1 - b_2 = 0 \quad (34)$$

$$2a_2 X_2 + b_2 - 2a_3 X_2 - b_3 = 0 \quad (35)$$

The above system of equations is put in matrix form as:

$$\begin{pmatrix}
 x & 1 & 0 & 0 & 0 & 0 & 0 & 0 \\
 0 & 0 & x_1^2 & x_1 & 1 & 0 & 0 & 0 \\
 0 & 0 & x_2^2 & x_2 & 1 & 0 & 0 & 0 \\
 0 & 0 & 0 & 0 & 0 & x_2^2 & x_2 & 1 \\
 x_0 & 1 & 0 & 0 & 0 & 0 & 0 & 0 \\
 0 & 0 & 0 & 0 & 0 & x_3^2 & x_3 & 1 \\
 1 & 0 & -2x & -1 & 0 & 0 & 0 & 0 \\
 0 & 0 & 2x_2 & 1 & 0 & -2x_2 & -1 & 0
 \end{pmatrix}
 \begin{pmatrix}
 b_1 \\
 c_1 \\
 a_2 \\
 b_2 \\
 c_2 \\
 a_3 \\
 b_3 \\
 c_3
 \end{pmatrix}
 =
 \begin{pmatrix}
 f(x_1) \\
 f(x_1) \\
 f(x_2) \\
 f(x_2) \\
 f(x_0) \\
 f(x_3) \\
 0 \\
 0
 \end{pmatrix}$$

The above system must be rearranged to avoid the presence of zero elements in leading diagonals. This avoids division by zero, when applying Gauss-Jordan method

2.3 Why Spline Modeling is Favoured: The responses of experimental results and viscoelastic materials are usually nonlinear as well as responses of viscoelastic materials. Therefore, a higher order polynomial is always expected of viscoelastic materials responses. A scatter plot of Ihueze [5] revealed nonlinear responses and a higher order polynomial fit. The critical stress - strain responses is shown in table 3 and fig. 3. Ihueze [5] used polynomial regression method to obtain a second order polynomial for a range of data of table 3. The standard error associated with this fit is 3.3469 while the correlation coefficient and coefficient of determination are 0.9828 and 0.9659 respectively. Spline functions are contemplated because splines fit a subset of

data points thereby reducing the error associated with interpolation within a wide range of data. The conventional interpolation fitting suggests that nth order polynomial fits n+ 1 data points. This suggests that the second order polynomial fitting of Ihueze [5] could be erroneous because he could have used 25th order polynomial for the 24 data points considered. This error is confirmed by the standard error of about 3 computed. 25th order fit will capture all the meandering suggested by the 24 points. However, this will lead to erroneous results because of round - off error and over shoot, Canale and Chapra [11]. An alternative approach is to apply lower - order polynomials to subsets of data points. Such connecting polynomials are called spline functions. To avoid the computational efforts of higher order splines, cubic spline is classically recommended, Kreys Zig [10] and Canale and Chapra [11].

Table 3 analysis of spline

Interval	X	Y(MPa)	Fi(x):Quad spline	Fi(x):Cub spline
0.024 ≤ x ≤ 0.036	0.024	25.71	25.709992	25.8057
	0.035	12.86	14.581655	14.5942
	0.036	13.57	13.569988	13.5727
0.036 ≤ x ≤ 0.061	0.036	13.57	13.56999	-1.1987
	0.048	8.46	5.5568	-11.88768
	0.061	6.19	6.18999	-23.9177
	0.061	6.19	6.1900	-11.7807
0.061 ≤ x ≤ 0.12	0.095	29.25	17.868078	-44.7553
	0.11	53.83	21.33844	-53.8313
	0.12	23.08	23.08	-61.7365

3 METHODOLOGY

Experimental and analytical methods were used.

3.1 Experimentation And Materials.

Hand Lay-up was used to form composites of F, G and H of approximately 4.8mm thick, 3.2mm thick and 3.1mm thick respectively as found in Ihueze [5]. The thickness of replicated samples of F, G and H are measured with micrometer screw gauge and 85 percentile was used to determine where about 85% of the measured thicknesses would fall. For F, G and H 85 percentile gave 4.8mm, 3.2 and 4.3 mm respectively. Replicated samples of A, B, C, D and E were subjected to axial compression in a Hounds field tensometer, and the Force deformation plot of the autographic recorder of the tensometer interpolated and recorded, the stress-strain response are also recorded in Ihueze [5].

3.2 Finite Element Method.

In the finite element method computer

subroutines were developed in visual basic to compute,

- (a) Nodes and assembly stiffness matrixes
- (b) Nodes thermal load and assembly thermal load vectors.

(c) The nodal degree of freedom or displacements at temperature range of 20 °C - 120°C. The minimum displacement or degree of freedom of nodes at the different temperatures computed from the assembly system of equations are used to predict the static strength of the composite sample from the data generated from experimental method i.e. using the compression force deformation and compression stress - strain responses of the experimental method. The predicted static stress - strain response of FEM is presented in table 1.

Table 1 Critical stress-strain at various temperatures

Critical strain X	Critical stress, Y (MPa)
0.024	25.71
0.024	22.14

0.036	25.71
0.024	25.71
0.036	13.57
0.035	12.86
0.036	13.57
0.036	13.57
0.061	6.19
0.048	8.46
0.061	6.19
0.061	6.19
0.11	53.85
0.095	29.29
0.11	50
0.11	50
0.12	23.08
0.11	50
0.12	23.08
0.12	23.08
0.12	23.08
0.12	23.08
0.12	23.08
0.12	23.08
0.12	23.08
0.12	23.08
0.12	23.08

Source: Ihueze [5] page 204

Table 1 is the stress strain response at temperature range of 20°C - 120°C at various moduli of composite samples. The flowchart that led to the programmes for the computation of FE results is shown in fig. 3 while the subroutine programmes are listed in appendix A of Ihueze [5].

It is the static stress - strain responses of FEM that is modeled by quadratic and cubic spline functions.

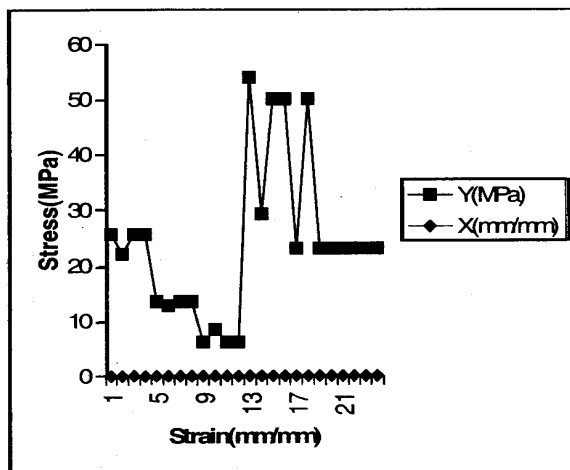


Fig. 4: Critical stress-strain graphics.

3.3 Modeling GRP Critical stress-strain Response

The methodology of this research work also involves the simulation of the system of equations developed by fitting cubic and quadratic polynomials to subset of data points, so that interpolation functions can be established for the limiting stresses of GRP composites working in the temperature range of 20 - 120°C. Subintervals are established for a range of data points as: $X_0 \leq x \leq X_1$, $X_1 \leq x \leq X_2$, $X_2 \leq x \leq X_3$ so that we have three interpolating functions as $f_1(x)$, $f_2(x)$, and $f_3(x)$ for the three intervals. **3.1 Estimation of Cubic Spline Coefficients and Modelling**

Ihueze [5] measured the critical stress strain response, of polyester matrix for GRP composites working in the temperature range of 20 - 120°C, using finite element method to generate numerical data. The critical stress-strain data is presented in table 1. Employing the intervals of data points,

$X_0 \leq x \leq X_1$, $X_1 \leq x \leq X_2$, $X_2 \leq x \leq X_3 = 0.024 \leq x \leq 0.036$, $0.036 \leq x \leq 0.061$, $0.061 \leq x \leq 0.12$. Putting the interval values in Eq. (5) through Eq. (6)-(17) and solving by Gauss-Jordan elimination:

$$a_1 = -7943.563, b_1 = 571.9365, c_1 = -1031.997, d_1 = 50.35401, a_2 = -31596.85, b_2 = 3126.491, c_2 = -984.1226, d_2 = 31.65196, a_3 = -16617.66, b_3 = 5982.358, c_3 = -1506.746, d_3 = 61.64238.$$

Putting these in Eq. (2)

$$f_1(x) = -7943.563 x^3 + 571.9365x^2 - 1031.997x + 50.35401 \quad (36)$$

$$f_2(x) = -31596.85 x^3 + 3126.491x^2 - 984.1226x + 31.65196 \quad (37)$$

$$f_3(x) = -16617.66x^3 + 5982.358x^2 - 1506.746x + 61.64238 \quad (38)$$

Where, x = Critical Strain, $f_1(x)$, $f_2(x)$, $f_3(x)$ = Critical stresses.

3.2 Estimation of Quadratic Spline.

Putting values in Eq. (16) and following similar procedures as in cubic spline:

$$a_1 = 0, b_1 = -1011.667, c_1 = 49.99, a_2 = 28658.67, b_2 = -3075.091,$$

$$c_2 = 87.13163, a_3 = -2288.059, b_3 = 700.4099, c_3 = -28.02113$$

The spline equations for the three intervals are therefore expressed as:

$$f_1(x) = -1011.667x + 49.99 \quad (39)$$

$$f_2(x) = 28658.67x^2 - 3075.091x + 87.13163 \quad (40)$$

$$f_3(x) = -2288.059x^2 + 700.4099x - 28.02113 \quad (41)$$

4 RESULTS AND DISCUSSION WITH SPLINES

4.1 Prediction with Splines

By putting the values of x in the spline Eqs. (1) to (6) Table 3.1 is obtained. Both x and y values of table 2 were extracted from table 1.

4.2 Optimization of Spline Models

Gradient search method was used to optimize the Spline functions to predict the critical parameters of stress and strain.

4.2.1 Optimization of cubic splines

The first and second derivatives of the cubic splines of Eqs. (36 to 38) gave the following equations.

$$f_1^1(x) = -23830.689x^2 + 1143.873x - 1031.997 \quad (42)$$

$$f_1^{11}(x) = -47661.378x + 1143.873 \quad (43)$$

$$f_2^1(x) = -94790.55x^2 + 6252.982x - 984.1226 \quad (44)$$

$$f_2^{11}(x) = -189581.1x + 6252.982 \quad (45)$$

$$f_3^1(x) = -49852.98x^2 + 11964.716x - 1506.746746 \quad (46)$$

$$f_3^{11}(x) = -99705.96x + 11964.716 \quad (47)$$

By equating Eq. (42), Eq. (43) and Eq. (44) to zero respectively the critical strains for the intervals were evaluated as 0.024, 0.03 and 0.12. These are used to calculate the critical stresses of the intervals as 25.81MPa, 4.1MPa and 61.74MPa, by putting the values of the critical strains computed back to Eqs. (36) - (38).

4.2.2 Optimization of Quadratic Spline

The first and second derivatives of Eq. (39) - (41) gave the following equations

$$f_1^1(X) = -1011.667 \quad (47)$$

$$f_1^{11}(X) = 0 \quad (48)$$

$$f_2^1(x) = 57317.34x - 3075.075.091 \quad (49)$$

$$f_2^{11}(x) = 57317.34 \quad (50)$$

$$f_3^1(x) = -4576.11Sx + 700.4099 \quad (51)$$

$$f_3^{11}(x) = -4576.118 \quad (52)$$

Following the procedures of section 4.2.1, the critical strains and stresses of the intervals are evaluated as 0.024, 0.054, and 25.71MPa, 4.65MPa, and 25.56MPa respectively. The sign of the value of the second derivative of a function establishes whether the function is a maxima or a minima, if sign of $f(x)^{11}$ is positive, then, $f(x)$ is a minima and if negative $f(x)$ is a maxima.

4.3 Discussion of Results

The graphics of fig. 5 and results of Eqs. (36)- (37) show that, limit stress decreases with strain increase at elevated temperatures before the commencement of strain hardening effects.

For the cubic spline, Eq. (42) predicted the critical strain for the cubic spline within the first interval as 0.024 and with Eq. (36) gives the limit or critical stress as 25.81MPa. Eq. (43) gives -0.000072 with $x = 0.024$. This means that the critical stress, 25.81MPa within the first interval is a maximum Eq. (44) predicted the critical strain for the cubic spline within the second interval, $0.036 < x < 0.06$ as 0.033 and with Eq. (37) gives 4.1MPa as limit stress. Eq. (45) with $x = 0.03$ gives -3.1943. This suggests a maxima. Eq. (46) predicted the critical strain for third interval as 0.12 and using this in equation (41), 61.74MPa is obtained. Eq. (47) with $x = 0.12$ gives 0.0008. This suggests a minima meaning that the functional value is maximum and decreases thereafter as the strain is increased.

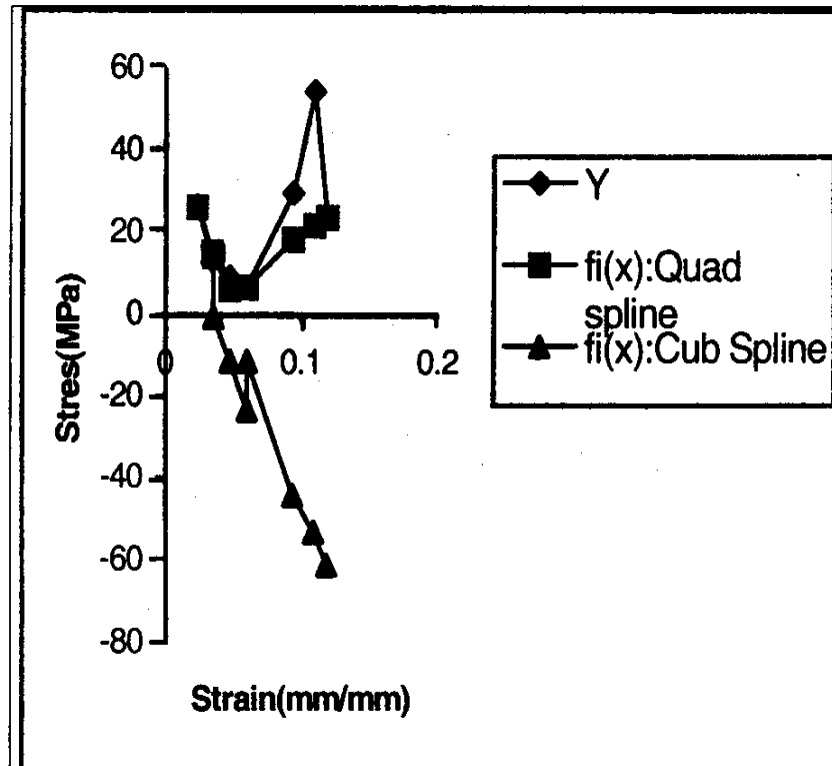


Fig. 5: Analysis of Spline graphics.

For the quadratic spline, fig. 5 gives the critical strain within the first interval as 0.024 and with this in equation (39) the critical stress is evaluated as 25.71MPa. Eq. (50) gives the sign of the second derivative of the function as positive; the value 25.71MPa predicted within the first interval by quadratic spline is therefore a minimum. Eq. (49) gives the critical strain for second interval as 0.054 and with equation (46) gives (4.65MPa) as the critical stress. The Sign of the value of Eq. (50) is positive. This suggests a minimum. Eq. (51) gives the value of the critical strain for the third interval as 0.15 and with this in equation (41) gives. 25.56MPa. The sign of the second derivative of the function is negative this suggests a maxima.

Minima and maxima describe the

minimum and maximum values of a function within an interval respectively. Therefore the minimum and maximum values of the function as predicted by cubic and quadratic splines depend greatly on strain.

Cubic spline analysis shows that after the lower critical strain of 0.024, the critical stress decreases until a strain of 0.033 when strain hardening picked to 0.12 giving critical stress of 61.74MPa. Strain hardening is therefore a strengthening process. The material exceeded the lower strength of 25.81MPa predicted by cubic spline within the third interval.

Quadratic spline analysis shows that after the lower critical strain of 0.024 the critical stress decreased until a strain of 0.054 when stress decreased to 4.65MPa

after which strain hardening picked at 0.15 with critical stress of 25.56MPa, which is a maxima.

5 CONCLUSION

26MPa is a limit stress predicted of first interval of splines, the models to be used for the prediction of stresses for strain range of 0.024-0.036 is therefore recommended as follows:

$$f_1(x) = -7943.563x^3 + 571.9365x^2 - 1031.997x + 50.334$$

$$f_1(x) = -1011.667x + 49.99$$

The optimum critical stress of this study is therefore in the range of 25.71MPa - 61.74MPa. The predictions of this work are considered correct when compared with a previous report for a typical stress - strain graph of plastics with 70°C operation. It is found that after a strain of 0.03 the strength decreases from 30MPa.

REFERENCES

1. Crawford, R.J., (1998), *Plastics Engineering*. 3rded, BUTTERWORTH HEINMANN, Oxford, 1998.
2. Budiansky, B. and Fleck, N.A, Compressive kinking of fibre composites, *Journal of Applied Mechanics*, ASME, Vol. 47, No.6, 1994, pp.246-249.
3. Chung, I. and Weitsmam, Y.J. Model for Micro-Buckling/Micro-Kinking Compressive Response of Fibre Reinforced Composites *ASME journal of Applied machine Vol. 47*, No. 6, 1994, pp.256-261.
4. Hsu, S.Y, Vogler, T.J. and Kyriakides, S. Compressive Strength Predication for Fibre Composites, *ASME Journal of Applied Mechanics*, Vol. 65, 1998, pp. 7-15.
5. Ihueze, C.C, Optimum Buckling Response Model of GRP Composites, Ph.D THESIS, UNN, 2005.
6. Wood, R, *Car Bodywork in Glass Reinforced Plastics*, PENTECH. Press, London: Plymouth, 1980.
7. Foye, J.F., Technical Report AFML - TR - 68 - 91, North America Rockwell Corporation, Columbus, OH., USA, 1965.
8. Enetanya, AN and Ihueze, C.C, Finite Element Thermal Analysis of GRP Auto Body Composite, *Journal of Science and Technical Research V3*, Number 4, 2004.
9. Argon, AS., *Fracture of Composites. Treatise of Material Science and Technology Vol. 1*. Academic Press, N.Y., 1972.
10. Kreyszig, E, *Advanced Engineering Mathematics*, 8th edition, John Wiley and Sons Publisher, New York, 2004.
11. Canale, R.P and Chapra, S.C, *Numerical Methods for Engineers*, McGraw-Hill Publishers, 3rd edition, Boston, N.Y., 1998

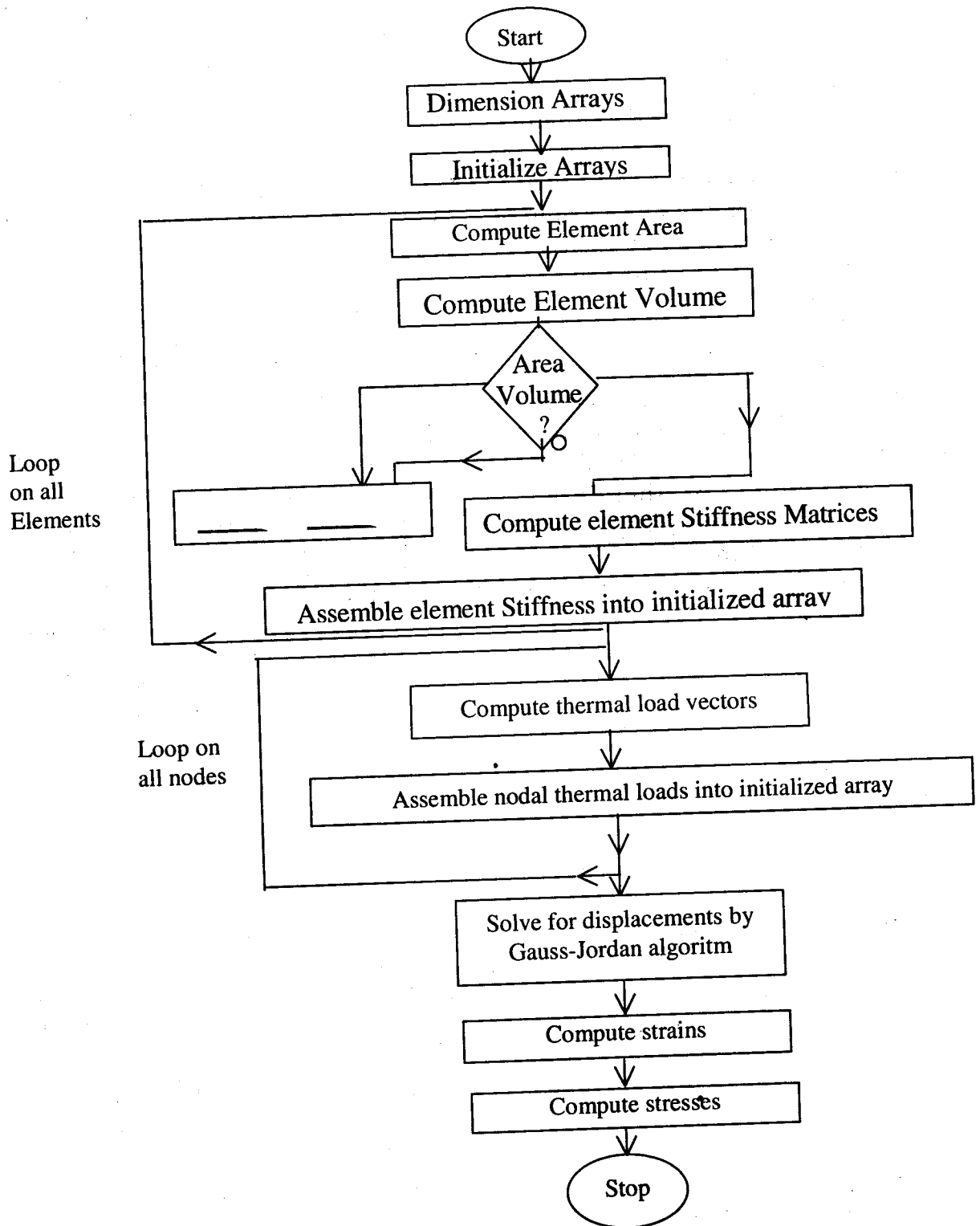


Fig. 3.2: Flow charat for computer implementation of FEM inV-basic.